Structural Engineering and Mechanics, *Vol. 49, No. 4 (2014) 463-477*
DOI: http://dx.doi.org/10.12989/sem.2014.49.4.463

Seismic performance evaluation and retrofitting with viscous fluid dampers of an existing bridge in Istanbul

Guliz Bayramoglu[*1], Alpay Ozgen[1a] and Enver Altınok[2b]

[1]*Faculty of Civil Engineering, Istanbul Technical University, 34469 Maslak-Istanbul, Turkey*
[2]*Altinok Consulting and Engineering, Darulaceze Street, 33/B-2, 34384, Okmeydani-Istanbul, Turkey*

(Received November 16, 2012, Revised December 9, 2013, Accepted December 27, 2013)

Abstract. In this paper, seismic performance of Kozyatagi Bridge is evaluated by employing nonlinear elasto-plastic dynamic analysis and the deformation-based performance. The time-history records of the 1999 Izmit, 1971 San Fernando and 1989 Loma Prieta earthquakes are modified by adopting a probability of exceedance of 2% in 50 years corresponding to the return period of 2475 years. The analysis is carried out for three different bearing cases which are movable bearings, restrained bearings, and movable bearings with viscous fluid dampers in the radial direction. The analysis results show that the bridge can be retrofitted with viscous fluid dampers. In this case the reinforced concrete piers need not be strengthened by any jacketing techniques in order to preserve the original architectural appearance of the bridge. The retrofitting design of the bridge with viscous fluid dampers is also presented in detail.

Keywords: nonlinear; elasto-plastic; dynamic analysis; deformation-based; time-history; retrofitting; viscous fluid damper

1. Introduction

Bridges, as one of the significant civil engineering structures, play an important main role in everyday life of the people in the metropolitan cities. Especially after earthquake disasters, serviceability of bridges becomes of high importance in order to help injured people and provide continuity of transportation. Major earthquake ground motions in the last two decades in the densely populated area had great impacts on many bridges (e.g., the 1994 Northridge earthquake, the 1995 Kobe earthquake, the 2007 Niigata earthquake); especially those designed according to the older codes and demonstrated that these structures are vulnerable. Therefore, it is needed to re-evaluate the seismic performance of the existing bridges according to the revised codes and specifications, and retrofit, if required.

Seismic isolation is one of the most effective techniques of retrofitting, to improve the seismic performance of the existing bridges (Sheikh *et al*. 2012, Avsar and Yakut 2012). Passive control

∗Corresponding author, Associate Professor, E-mail: güliz.bayramoglu2@itu.edu.tr
[a]Professor, E-mail: ozgena@itu.edu.tr
[b]Civil Engineer, E-mail: altinokconsult@yahoo.com

http://www.techno-press.org/?journal=sem&subpage=8 ISSN: 1225-4568 (Print), 1598-6217 (Online)

devices such as viscous fluid dampers, viscoelastic solid dampers, friction dampers, and metallic dampers are commonly used for seismic retrofitting of the existing bridges. However, retrofitting by the use of viscous fluid dampers is a way of adding high-energy dissipation in the lateral motion of a bridge without involving major construction modification.

Studies and applications on passive control techniques with viscous fluid dampers to buildings and bridges as well as mathematical modeling of their dynamic response have greatly increased in recent years. Symans *et al.* (2008) have presented a summary of current practice and recent developments in the application of passive energy dissipation systems for seismic protection of structures. Furthermore, emphasis is placed on descriptions of viscous, viscoelastic, metallic, and friction damping systems, including recent applications of such systems. Madhekar and Jangid (2010) have investigated the performance of variable dampers for seismic protection of the benchmark highway bridge under six real earthquake ground motions using a velocity-dependent damping model of variable damper. The results of these investigations clearly indicate that the base shear, the base moment and the mid-span displacement can be substantially reduced. Lee and Taylor (2002) have described the fluid damper technology, analysis considerations, and some installation methods. Hwang and Tseng (2005) have suggested an application of the nonlinear viscous dampers for controlling excessive vibrations that will ultimately lead to significant damage that affects not only the serviceability but also the structural integrity of the bridge system. Martinez-Rodrigo, Lavado and Museros (2010) have proposed and evaluated the possibility of retrofitting two short simply supported existing railway bridges with viscous fluid dampers connected to the deck slab and to an auxiliary structure in order to reduce their dynamic responses under the circulation of high-speed traffic. Kandemir *et al.* (2011) have investigated the retrofitting process of an existing upper-deck type steel arch bridge. By using the nonlinear dynamic response analysis, the seismic performance evaluation of the bridge is upgraded by viscous dampers with velocity dependency under major earthquakes. Soneji and Jangid (2007) have carried out the performance of passive hybrid control systems used for the earthquake protection of a cable-stayed bridge under real earthquake ground motion. A viscous fluid damper is used as a passive supplemental energy dissipation device in association with elastomeric and sliding isolation systems to form a passive hybrid control system. Museros and Martinez-Rodrigo (2007) have presented and numerically evaluated a new alternative for reducing the resonant vibration of simply supported beams under moving loads. The strategy proposed is based on the use of linear fluid viscous dampers that connect the main beam carrying the loads and an auxiliary beam placed underneath the main one. Dion *et al.* (2011) have proposed a real-time dynamic substructuring test program carried out on an existing bridge structure equipped with two innovative viscous seismic protective devices: a seismic damping unit and a shock transmission unit. The results of the tests that were run under various ground motions indicate that simple numerical modeling techniques can lead to accurate prediction of the displacement response of bridge structures equipped with the seismic protective system studied.

After the 1999 Izmit earthquake, retrofitting of some important bridges and viaducts in metropolitan city Istanbul has become a current issue. Kozyatagi Bridge located on the Anatolian side of Istanbul is one of them. In this paper, seismic performance of Kozyatagi Bridge is evaluated based on nonlinear elasto-plastic dynamic analysis, and also the retrofitting design of the bridge with viscous fluid dampers is presented in detail.

2. Description of Kozyatagi Bridge and the site characteristics

Kozyatagi Bridge built in 1986 is a highway connection bridge with a total length of 409.60 m, and has 11 spans with a maximum span of 41.80 m between the piers (Fig. 1). As shown in Fig. 2, the bridge alignment descending from level 84.209 m in the north abutment to level 73.863 m in the south abutment is curved in a circular arc with a radius of curvature of 280 m, measured from the origin of the circular arc to the centre-line of the composite superstructure. The bridge was originally designed as a one way bridge with double lanes for the live load class of H30-S24 according to AASHTO (1983).

The composite superstructure consists of a reinforced concrete deck and a semi-elliptical steel hollow cross-section. The cross-sectional details of the composite superstructure are shown in Fig. 3. The reinforced concrete deck has a width of 14.0 m and an average thickness of 225 mm which increases to 325 mm at its connection to the steel hollow cross-section, and the concrete quality is C30. On the other hand, the steel hollow cross-section is a height of 1.70 m at the middle of the cross-section, and the steel quality is S235. The wall thickness of the steel hollow cross-section varies between 10 mm and 12 mm along the bridge, and is stiffened with transverse and

Fig. 1 A view of Kozyatagi Bridge

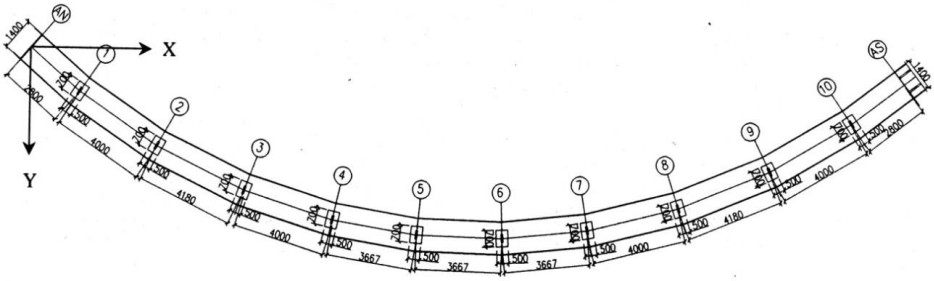

(a) Plan view

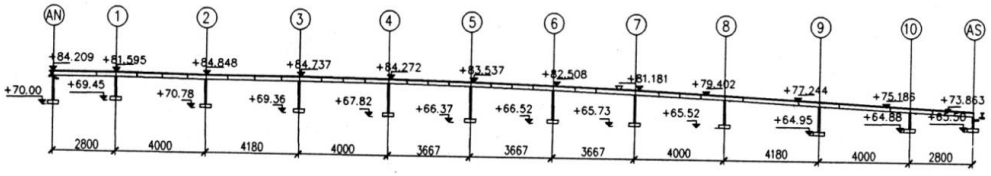

(b) Elevation view

Fig. 2 Kozyatagi bridge (all dimensions in mm)

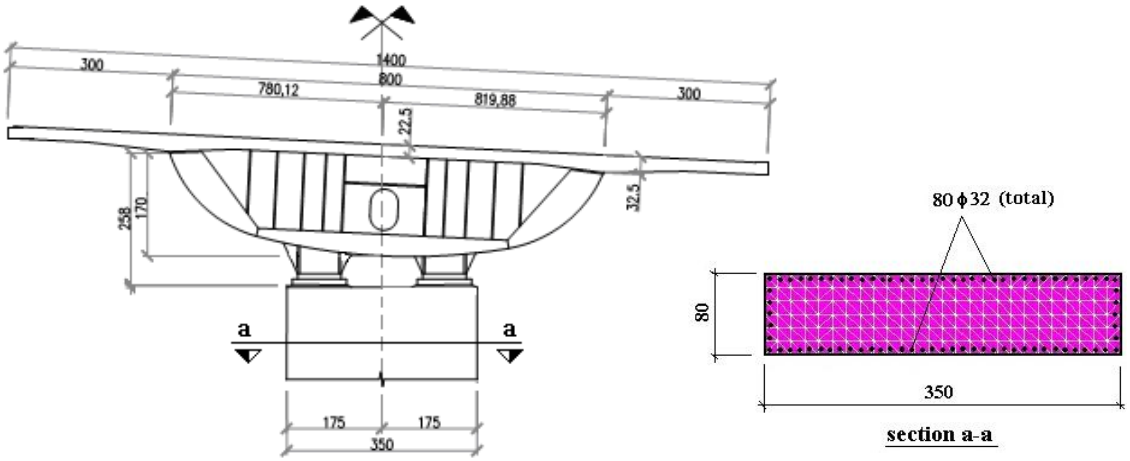

Fig. 3 The cross-sections of the superstructure and the piers (all dimensions in cm)

Fig. 4 Steel bearings of the superstructure

longitudinal stiffeners at the bearing and opening locations of the bridge. The concrete deck has a cantilever of 3.0 m on both sides. The composite action between the concrete deck and the steel web is provided by steel studs with a diameter of 20 mm, a height of 150 mm and a steel quality of S275.

The reinforced concrete piers have a rectangular cross-section of 0.80 m × 3.50 m, and their heights vary between 9.756 m and 16.617 m. The concrete quality is determined as C25 by testing on the concrete core specimens taken out from the piers (Tasdemir 2006). All the piers are supported on the spread plate foundations with a dimension of 7.0 m × 7.0 m × 1.5 m.

The superstructure is supported on each pier with two steel bearings. The trapezoidal steel bearing plates of 60 mm thickness are welded to the bottom of steel hollow cross-section, and are stiffened with three 12 mm thick steel plates at the both surfaces, as shown in Fig. 4. The bearing plates are seated into slots made of cast steel at the top of the piers. Thus, all the bearings are movable in the radial direction, while the intermediate bearings are restrained and the end bearings are movable in the longitudinal direction to the curved superstructure.

According to the geotechnical inspections (Altinok Consulting 2007), the soil on which the foundations are supported has rock characteristics with an ultimate soil pressure of q_u = 1.80

MN/m^2, a bedding coefficient of 286 MN/m^3 and a shear wave velocity of 335 m/s. No groundwater is found in the soil.

3. Nonlinear dynamic analysis of the bridge

3.1 Assumptions

In this paper, the following assumptions are made for the nonlinear analysis of the bridge:

• The composite superstructure and the concrete piers are modeled using 2D beam_elements, and the masses are defined to be distributed along the axes of the beam elements.

• The superstructure is assumed to remain elastic during seismic excitation due to the high bending rigidity.

• The friction forces in the movable bearings are neglected.

• The piers are rigidly fixed to the foundation plates.

• Earthquake ground motions are considered in two horizontal directions, *X* and *Y*, perpendicular to each other.

• The seismic performance of the bridge is evaluated by considering the deformation-based performance design.

• For the structural model, the plastic hinges are inserted at the lower end cross-sections of each pier.

3.2 Loads and structural system

The weight of the composite superstructure including the concrete deck, asphalt coat, steel hollow cross-section, steel bearings, balustrade and the other components is determined as 114.3 kN/m.

The bridge structure is modeled and analyzed by using software SAP2000. In the structural system, the composite superstructure and the concrete piers are modeled using 2D beam elements, and the masses are defined to be distributed along the axes of the beam elements. The superstructure is connected to the piers with massless rigid bars as shown in detail *A* in Fig. 5. The piers are rigidly fixed to the foundation plates supported on soil.

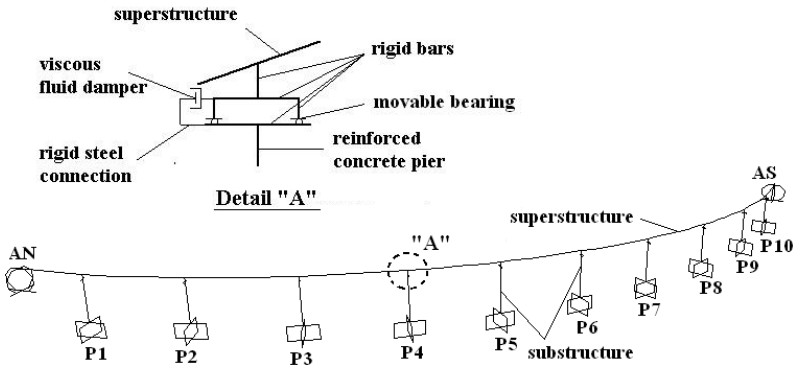

Fig. 5 Structural system and modeling of bearings with viscous fluid dampers

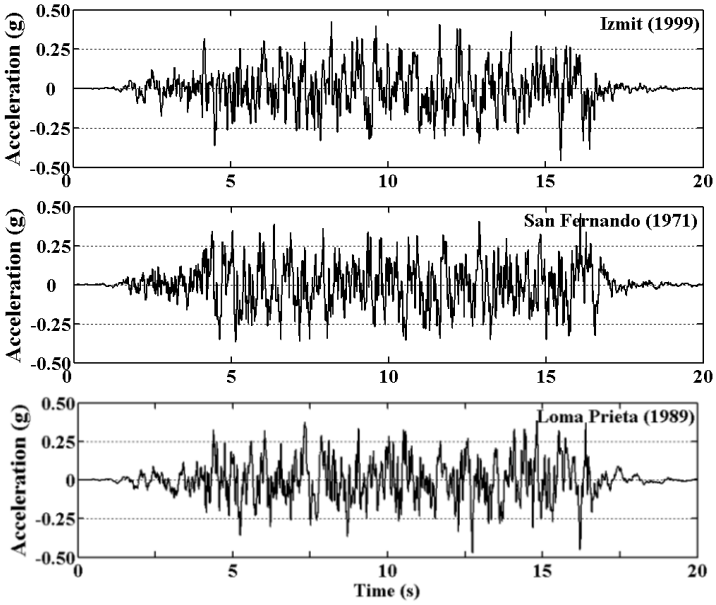

Fig. 6 Modified ground motion records used in the analysis

3.3 Performance criteria

The seismic performance of the bridge is evaluated by considering the deformation-based performance design (Aydinoglu 2005). In this procedure, a structural damage is expected under a maximum probable earthquake. It is also assumed that certain elements of the bridge can experience significant nonlinear deformations during this earthquake motion; however the damage should not affect the overall stability of the bridge, and can be repaired in a reasonable time.

3.4 Time-history records of the earthquakes considered

The nonlinear dynamic performance evaluation is assessed through the time-history analysis. The time-history records of the 1999 Izmit, 1971 San Fernando and 1989 Loma Prieta earthquakes are considered and modified to represent the seismic and site characteristics of the bridge location for a probability of exceedance of 2% in 50 years corresponding to the return period of 2475 years (Ipek 2005). The time-history seismic records of these three earthquakes are shown in Fig. 6.

3.5 Material characteristics and section properties of the structural system

The material characteristics of the concrete deck and the steel hollow cross-section, and also the section properties of the composite superstructure are given in Table 1 and Table 2, respectively.

The characteristics of the unconfined concrete of C25 (Mander, Priestly and Park 1988) and the strain-hardening reinforcement steel of S420 (TEC 2007) are used in modeling of the piers (Figs. 7 and 8). There are longitudinal reinforcements of 80 ϕ32 at the piers. The modulus of elasticity of the concrete is assumed to be 23650 MPa.

Table 1 Material characteristics of the composite superstructure (MPa)

Material characteristics	Concrete deck	Steel hollow cross-section
Compressive strength	30	--
Yield strength	--	235
Ultimate tensile strength	--	360
Modulus of elasticity	25900	210000

Table 2 Section properties of the composite superstructure

Cross-sectional area	Moment of inertia		Torsion constant
	strong axis	weak axis	
0.6348 m^2	9.0893 m^4	0.2713 m^4	1.6887 m^4

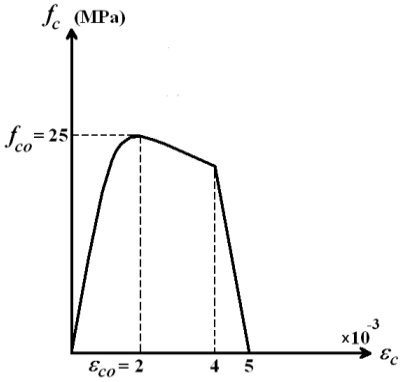

Fig. 7 Stress-strain relation of the unconfined concrete

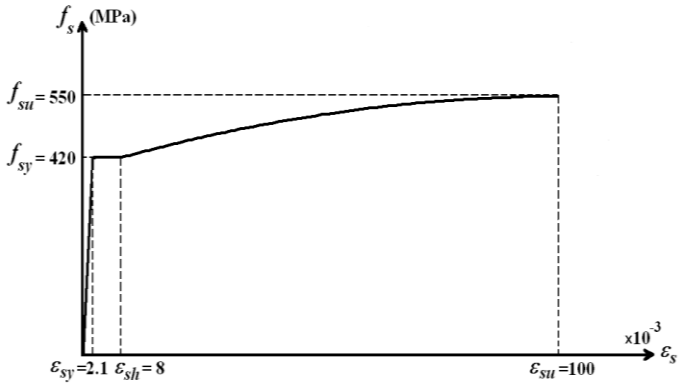

Fig. 8 Stress-strain relation of the reinforcement steel

3.6 Modeling of nonlinear behavior of the bridge

The traditional plastic hinge hypothesis is adopted in the modeling and the evaluation of the nonlinear behavior of the bridge (Priestly *et al.* 1996). This hypothesis is based on the assumption that the plastic deformations are lumped at certain section of the structural element and can be assumed to be constant in these sections. The plastic hinges are inserted in the middle of these regions, and the other parts of the structural element are assumed to behave linearly elastic. As the piers are cantilevered and have uniform cross-section and uniform reinforcement, the plasticization will clearly take place at the lower end cross-sections of each pier where the maximum moment will occur. The plastic hinge lengths are defined in these locations as follows (CALTRANS 2004)

$$L_p = 0.08\,H + 0.022\,f_y\,d_b \geq 0.044\,f_y\,d_b \tag{1}$$

where H is the pier height (mm), f_y is the yield strength of the reinforcement steel (MPa), and d_b is the diameter (mm) of the longitudinal reinforcement. In the present case the plastic hinge lengths vary between 1076 mm and 1625 mm due to the variation in the height of the piers. For the structural model, the plastic hinges are inserted at the lower end cross-sections of each pier.

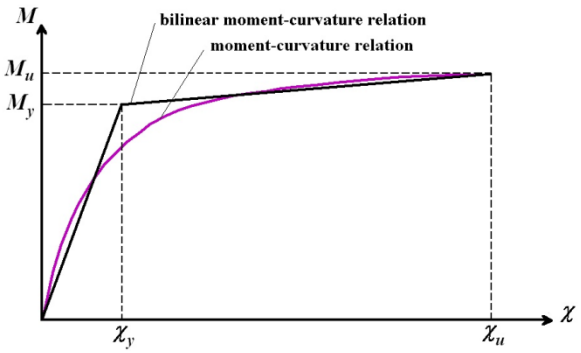

Fig. 9 Typical moment-curvature curves

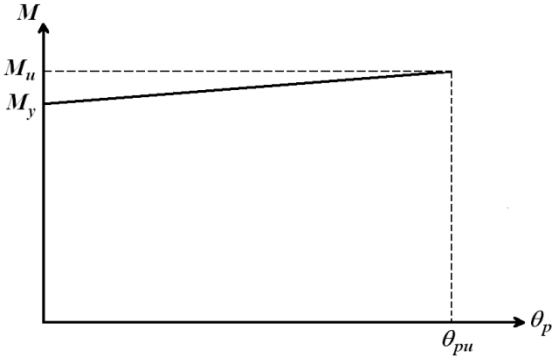

Fig. 10 Typical moment-plastic rotation curve

Table 3 Yield and ultimate moments and plastic rotations of the piers

Pier	Axial force	Yield moment		Ultimate moment		Plastic rotation $\times 10^{-3}$	
	N (kN)	$M_{y,x}$ (kNm)	$M_{y,y}$ (kNm)	$M_{u,x}$ (kNm)	$M_{u,y}$ (kNm)	$\theta_{pu,x}$ (rad)	$\theta_{pu,y}$ (rad)
P1	5242	42220	10680	42300	11810	5.1	39.0
P2	5713	42740	10840	42800	11910	4.8	36.3
P3	5757	42800	10860	42810	11920	5.1	39.0
P4	5457	42460	10750	42470	11850	5.5	42.1
P5	5309	42300	10700	42400	11820	5.7	44.1
P6	5231	42210	10670	42300	11800	5.4	41.8
P7	5391	42380	10730	42400	11840	5.2	40.2
P8	5661	42690	10820	42700	11900	4.7	36.1
P9	5596	42610	10800	42700	11880	4.3	32.9
P10	4940	41880	10570	42000	11740	3.9	29.9

3.7 Moment-curvature and moment-plastic rotation curves

Considering the axial forces due to the gravity loads, moment-curvature ($M-\chi$) curves are plotted by using software XTRACT for the lower end cross-sections of each pier, where the plastic hinge is expected to form; and these curves are then converted to bilinear ($M-\chi$) curves. Typical ($M-\chi$) and bilinear ($M-\chi$) curves are shown in Fig. 9. Moment-plastic rotation ($M-\theta_p$) curves are obtained from the bilinear ($M-\chi$) curves. A typical ($M-\theta_p$) curve is shown in Fig. 10. The yield and ultimate moments and the plastic rotations for each pier are given for both strong and weak axes in Table 3.

The effective stiffnesses of the cracked cross-sections of the piers are also obtained by the same software. These stiffnesses vary between 32.0×10^6 kNm^2 and 32.5×10^6 kNm^2 for strong axis, between 2.21×10^6 kNm^2 and 2.23×10^6 kNm^2 for weak axis. The cracked bending rigidities of the pier sections correspond to M_y/χ_y in Fig. 9.

3.8 Viscous fluid dampers

The viscous fluid dampers used for retrofitting of the bridge have a maximum stroke of ±100

mm and a capacity of 1000 kN. The damping force is produced from viscous fluid passing through an orifice from one chamber to another chamber in a cylindrical volume. The force–velocity relationship of the viscous damper is assumed to be expressible as (Farzad and Kelly 1999)

$$F = C\ V^{\alpha} \tag{2}$$

where F is the viscous damping force, C is the viscous damping coefficient, V is the relative velocity between two ends of damper and α is the damping exponent. In the analysis, it is assumed that $C = 2000$ kN s/m and $\alpha = 0.6$.

4. Evaluation of the seismic performance of the bridge

To determine the seismic performance of the bridge, the analysis is carried out for three different bearing cases: (1) movable bearings, (2) restrained bearings, and (3) movable bearings with viscous fluid dampers in the radial direction.

The differential equation of earthquake motion for the bridge is given by the following equation (Chopra 2001)

$$\mathbf{m}\,\ddot{\mathbf{u}} + \mathbf{c}\,\dot{\mathbf{u}} + \mathbf{k}\,\mathbf{u} = -\mathbf{m}\,\mathbf{1}\,\ddot{u}_g(t) \tag{3}$$

where **m**, **c** and **k** represent the mass, damping and stiffness matrices, respectively, while $\ddot{\mathbf{u}}$, $\dot{\mathbf{u}}$, and **u** denote the structural acceleration, velocity and displacement vectors, respectively. **1** is an unit vector, $\ddot{u}_g(t)$ is the horizontal ground acceleration. Although this equation system seems to be linear, it is in fact nonlinear due to variation of stiffnesses and due to nonlinear damping force. This nonlinear differential equation system is solved by direct integration using the Wilson's method. The nonlinear elasto-plastic dynamic analysis is performed using the $(M-\chi)$ curves at the plastic hinge sections in SAP2000 for the three time-history seismic records in two horizontal directions, X and Y separately. X-direction is in the longitudinal direction which connects two abutments, and Y, the transverse direction, is perpendicular to X.

In the analysis, the friction forces in the movable bearings are neglected. In FEMA 356 and Aydinoglu (2005), the allowable strain limits are given as $\varepsilon_c = 0.004$ for the unconfined concrete, and $\varepsilon_s = 0.06$ for the reinforcement steel. However, these values are decreased by 2/3 to $\varepsilon_c = 0.0027$ and $\varepsilon_s = 0.04$ as an additional safety by 17th Region Office of General Directorate of Highways in Turkey.

4.1 Movable bearings (existing bridge)

The analysis results show that excessive relative transverse displacements have occurred at the movable bearings between the composite superstructure and the concrete piers. Thus, in the subsequent analysis case, the relative displacements are considered to be restrained completely by stoppers in the radial direction.

4.2 Restrained bearings

In this analysis case, large internal forces have been developed in the concrete piers. The plastic deformations have taken place at the lower end cross-sections of piers P8 to P10 at the Izmit and

San Fernando earthquakes in *X*-direction, piers P9 and P10 at the Loma Prieta earthquake in *X*-direction, piers P1 to P7 at the Izmit and Loma Prieta earthquakes in *Y*-direction, piers P1 to P7 and P10 at the San Fernando earthquake in *Y*-direction. In this case, the plastic deformations have not exceeded the strain limit for the reinforcement steel in any pier; but they have approached the strain limit for the unconfined concrete for the other piers, except for piers P3, P4 and P6. The strain values have exceeded the limit value with a strain of $2.948\text{x}10^{-3}$ in pier P6 at the Izmit earthquake, with strains of 2.975×10^{-3} and 2.768×10^{-3}, respectively, in piers P3 and P4 at the Loma Prieta earthquake in Y-direction.

The soil pressures under the pier foundations have not exceeded the allowable soil pressure, but the foundation plates have separated from the soil excessively. The dimensions of the foundations are found to be insufficient. Consequently, it is decided that the foundations and the piers need retrofitting in this case.

4.3 Bearings with viscous fluid dampers (retrofitted bridge)

By the viscous fluid dampers mounted on top of the concrete piers, the relative transverse displacements at the bearings and the internal forces at the piers and the foundations have been reduced, and thus there are no plastic deformations at the lower end cross-sections of all the piers for the earthquake actions in *Y*-direction and these are decreased in *X*-direction. The deformations at the lower end cross-sections of the piers are summarized in Table 4. As seen from Table 4, very

Table 4 Evaluation of the seismic performance of the piers for the retrofitted bridge

	$\chi_y\times10^{-3}$ (rad/m)	$\theta_p\times10^{-3}$ (rad)	L_p (mm)	$\chi_p\times10^{-3}$ (rad/m)	$(\chi_y+\chi_p)\times10^{-3}$ (rad/m)	$\varepsilon_c\times10^{-3}$	$\varepsilon_s\times10^{-3}$
Pier P1							
LPR-X	4.811	0.170	1432	0.119	4.930	1.146	2.640
Pier P2							
SFR-X	4.860	1.572	1377	1.142	6.002	1.260	3.189
LPR-X	4.860	2.133	1377	1.549	6.409	1.350	3.735
Pier P8							
SFR-X	4.855	1.718	1362	1.261	6.116	1.257	3.189
LPR-X	4.855	2.682	1362	1.969	6.824	1.347	3.734
Pier P9							
IZM-X	4.848	1.651	1235	1.337	6.185	1.254	3.187
SFR-X	4.868	4.877	1235	3.948	8.796	1.489	4.855
LPR-X	4.848	5.966	1235	4.830	9.678	1.569	5.568
Pier P10							
IZM-X	4.780	6.105	1076	5.673	10.453	1.602	6.347
SFR-X	4.780	9.371	1076	8.708	13.487	1.725	7.894
LPR-X	4.780	10.523	1076	9.778	14.558	1.764	8.690

χ_y: Yield curvature; θ_p: Plastic rotation; L_p: Plastic hinge length; χ_p: Plastic curvature; ε_c: Strain for the unconfined concrete; ε_s : Strain for the reinforcement steel; IZM-X: The 1999 Izmit earthquake in longitudinal direction; LPR-X: The 1989 Loma Prieta earthquake in longitudinal direction; SFR-X: The 1971 San Fernando earthquake in longitudinal direction

small plastic deformations have occurred at the lower end cross-sections of piers P9 and P10 at the Izmit earthquake, piers P2 and P8 to P10 at the San Fernando earthquake, piers P1, P2 and P8 to P10 at the Loma Prieta earthquake in *X*-direction. Also these plastic deformations have not exceeded the strain limits for the reinforcement steel and for the unconfined concrete in each pier.

The maximum damping forces and the maximum damper movements obtained in the analysis are shown in Fig. 11(a) and (b), respectively. As seen, the maximum damping force and the maximum damper movement have occurred in pier P6 with values of 992 kN and 78 mm, respectively, at the San Fernando earthquake in Y-direction, and these values remain within the capacity limits of the viscous fluid dampers. For the same earthquake motion, the damping force–time and damper movement–time variations in pier P6 are also shown in Fig. 12(a) and (b), respectively.

The maximum displacements at the abutments are obtained as 150 mm at the San Fernando and Loma Prieta earthquakes in X-direction, and 80 mm at the Izmit earthquake in Y-direction.

The analysis shows that all the piers of the retrofitted bridge have sufficient shear capacity. The maximum soil pressures under the pier foundations are determined as 887 $kN/m^2 < 1200\ kN/m^2$ and 801 $kN/m^2 < 1200\ kN/m^2$, at the Loma Prieta earthquake in X- and Y-directions, respectively. The

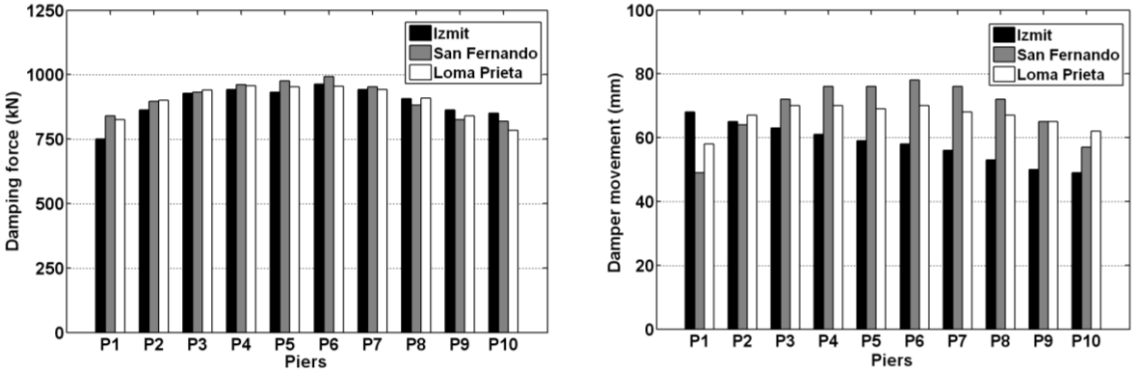

(a) Maximum damping forces (b) Maximum damper movements

Fig. 11 Time history response of viscous fluid dampers

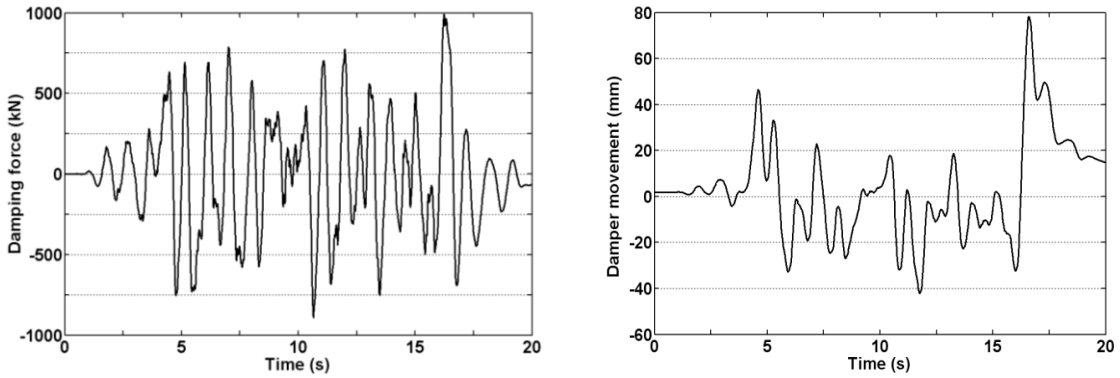

(a) Damping force–time variations (b) Damper movement–time variations

Fig. 12 Time history response of pier P6 at the San Fernando earthquake in Y-direction

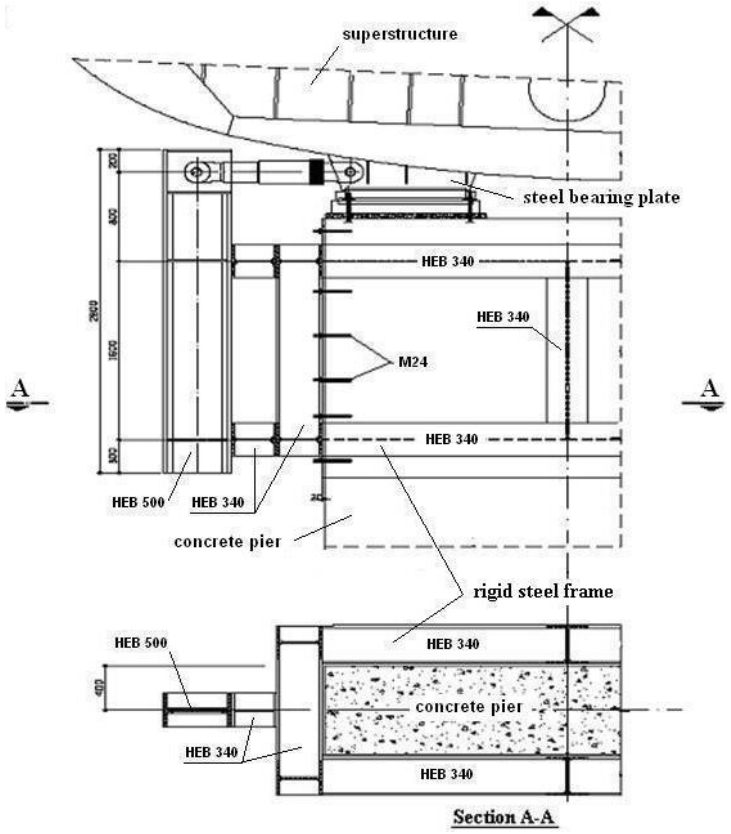

Fig. 13 Connection detail of the viscous fluid dampers to the superstructure and the piers

foundation plates are adequate in dimension. They have sufficient bending, shear and punching strengths for all earthquakes in both directions.

5. Retrofitting of the bridge with viscous fluid dampers

In the retrofitting strategy, 17th Region Office of the General Directorate of Highways in Turkey demands that the concrete piers should not be modified by any jacketing techniques in order to preserve the original architectural appearance of the bridge. In addition to that the continuity of transportation should not be prevented during the retrofitting works, since traffic is heavy on this connection bridge and the highway passing under it. Therefore, it is agreed that the bridge should be retrofitted with viscous fluid dampers. The dampers are connected to one of the existing steel bearing plates welded to the superstructure and to the rigid steel frames fixed to the top of the piers in the radial direction (Fig. 13). The dampers are placed in the middle of the narrower sides of the piers. For this purpose the following steps of action are carried out:

First, the top end of each pier is covered by 20 mm thick steel plates for a length of 2.325 m. Then the horizontal HEB 340 profiles are welded with fillet and butt welds all around to these steel plates and to each other at the top and bottom sides. These profiles are also connected to each other

by vertical HEB 340 profiles at each corner and at the middle of the wider sides of the pier. The viscous fluid damper is then attached to 60 mm thick steel bearing plate and to the vertical HEB 500 profile supported on the rigid steel frame by means of two pieces of HEB 340 profiles. At the connection of the damper to the vertical HEB 500 profile, one flange and the web of HEB 500 profile are cut out, and two 25 mm thick plates are welded instead of the web; the connecting pin of the damper goes in between the two plates.

The vertical HEB 500 profile is designed as a cantilevered beam with a span length of 1.60 m and a cantilever length of 0.80 m, subjected to a maximum damper force of 1000 kN at the end of the cantilever.

The calculated maximum stress for profiles is 187 MPa, which is within safety limit.

6. Conclusions

In this paper, seismic performance of Kozyatagi Bridge is evaluated based on nonlinear elasto-plastic dynamic analysis. Retrofitting design of the bridge with viscous fluid dampers is also presented in detail. The modified acceleration time-history records of the 1999 Izmit, 1971 San Fernando and 1989 Loma Prieta earthquakes are used to assess the seismic performance of the bridge. The nonlinear dynamic analysis is carried out for three different bearing cases: (1) movable bearings, (2) restrained bearings, and (3) movable bearings with viscous fluid dampers in the radial direction.

In the first analysis, that is the movable bearing case, excessive relative transverse displacements have occurred between the composite superstructure and the concrete piers. In the second analysis, that is the restrained bearing case, the relative displacements are considered to be restrained by stoppers in the radial direction. However, large internal forces have been found to develop in the concrete piers. The plastic deformations have accused at the lower end cross-sections of most piers. Although these plastic deformations have not exceeded the strain limit for the reinforcement steel in any of the piers, they have approached the allowable limit of strain for the unconfined concrete in some piers, and exceeded the limit value only in a few piers. In this case, although the soil pressures under the pier foundations have not exceeded the allowable soil pressure, the foundation plates have separated from the soil excessively. The dimensions of the foundations are found to be insufficient. Consequently, the foundations and the piers need retrofitting.

In the retrofitting strategy, the viscous fluid dampers are mounted on top of the piers in the radial direction. Thus, the relative transverse displacements at the bearings are limited, and the internal forces at the piers and the foundations are also reduced.

From the nonlinear dynamic analysis of the bridge retrofitted with viscous fluid dampers, the following conclusions are drawn:

- In very few piers, very small plastic deformations have occurred.
- The strain limits have not exceeded for the unconfined concrete and the reinforcement steel in any of the piers.
- All the piers have sufficient shear capacity.
- The soil stresses under the pier foundations are in safety limits.
- The foundation plates are adequate in dimension. They have sufficient bending, shear and punching strengths for all earthquakes in both directions.
- The viscous fluid dampers are sufficient to control the seismic vibration response of the

bridge.

• The maximum damping force and the maximum damper movement are achieved in pier P6 with values of 992 kN and 78 mm, respectively.

• The maximum displacements at the abutments are obtained as 150 mm and 80 mm in *X*- and *Y*-directions, respectively.

The following conclusions are drawn for the presented retrofitting design:

• The concrete piers need not be modified by any of the jacketing techniques in order to preserve the original architectural appearance of the bridge.

• The retrofitting work is carried out without disturbing the transportation on the bridge and the traffic on the highway.

• There is no reduction in the current strength of the bridge due to retrofitting works.

Acknowledgments

The authors gratefully acknowledge the technical information of this study by 17th Region Office of the General Directorate of Highways in Turkey and also Altinok Consulting Engineering staff for providing it.

References

AASHTO (1983), *Standard Specifications for Highway Bridges*, American Association of State Highway and Transportation Officials, Washington, DC.

Altinok Consulting Müh. Taahhüt San. ve Tic. Ltd. Şti. (2007), "Geotechnical Report of the Kozyatagi Bridge", Istanbul.

Avsar, O. and Yakut, A. (2012), "Seismic vulnerability assessment criteria for RC ordinary highway bridges in Turkey", *Struct. Eng. Mech.*, **43**(1), 127-145.

Aydinoglu, M.N. (2005), "The seismic performances of bridges and viaducts which exist or retrofit using nonlinear analysis methods", Technical Report, Istanbul.

CALTRANS (2004), *Seismic Design Criteria*, California Department of Transportation, Sacramento, California.

Chopra, A.K. (2001), *Dynamics of Structures, Theory and Applications to Earthquake Engineering*, Prentice-Hall Inc., New Jersey, USA.

Dion, C., Bouaanani, N., Trembly, R., Lamarche, C.P. and Leclerc, M. (2011), "Real-time dynamic substructuring testing of viscous seismic protective devices for bridge structures", *Eng. Struct.*, **33**(12), 3351-3363.

Farzad, N. and Kelly, J.M. (1999), *Design of Seismic Isolated Structures*, John Wiley & Sons Inc., New York, USA.

FEMA 356 (2002), *Prestandard and Commentary for the Seismic Rehabilitation of Buildings*, Federal Emergency Management Agency, Washington DC.

Ipek, M. (2005), "Repairing and seismic retrofitting of the bridges and viaducts on the highways and the connection ways", Seismic Report, 17th Region Office of the General Directorate of Highways in Turkey, Istanbul.

Hwang, J.S. and Tseng, Y.S. (2005), "Design formulations for supplemental viscous dampers to highway bridges", *Earthq. Eng. Struct. Dyn.*, **34**(13), 1627-1642.

Kandemir, E.C., Mazda, T., Nurui, H. and Miyamoto, H. (2011), "Seismic retrofit of an existing steel arch bridge using viscous damper", *Procedia Eng.*, **14**, 2301-2306.

Lee, D. and Taylor, D.P. (2002), "Viscous damper development and future trends", *Struct. Des. Tall Build.*, **10**(5), 311-320.
Madhekar, S.N. and Jangid, R.S. (2010), "Seismic response control of benchmark highway bridge using variable dampers", *Smart Struct. Syst*., **6**(8).
Mander, J.B., Priestley, M.J.N. and Park, R. (1988), "Theoretical stress-strain model for confined concrete", *J. Struct. Div., ASCE*, **114**(8), 1804-1826.
Martinez-Rodrigo, M.D., Lavado, J. and Museros, P. (2010), "Dynamic performance of existing high-speed railway bridges under resonant conditions retrofitted with fluid viscous dampers", *Eng. Struct*., **32**(3), 808-828.
Museros, P. and Martinez-Rodrigo, M.D. (2007), "Vibration control of simply supported beams under moving loads using fluid viscous dampers", *J. Sound Vib.*, **300**(1-2), 292-315.
Priestly, M.J.N., Seible, F. and Calvi, G.M. (1996), *Seismic Design and Retrofit of Bridges*, John Wiley & Sons Inc., New York, USA.
SAP2000-V.10.0.5. Structural Analysis Program, Computers & Structures Inc., California.
Sheikh, M.N., Xiong, J. and Li, W.H. (2012), "Reduction of seismic pounding effects of base-isolated RC highway bridges using MR damper", *Struct. Eng. Mech.*, **41**(6), 791-803.
Soneji, B.B. and Jangid R.S. (2007), "Passive hybrid systems for earthquake protection of cable-stayed bridge", *Eng. Struct.*, **29**(1), 57-70.
Symans, M.D., Charney, F.A., Whittaker A.S., Constantinou, M.C., Kircher, C.A., Johnson M.W. *et al.* (2008), "Energy dissipation systems for seismic applications: Current practice and recent developments", *J. Struct. Eng., ASCE*, **134**(1), 3-21.
Tasdemir, M.A. (2006), "Repairing and seismic retrofitting projects of the bridges on the highways and the connection ways", Material Evaluation Report at Istanbul Technical University, Istanbul.
TEC (2007), *Specification for Structures to be Built in Disaster Areas*, Turkish Earthquake Code, The Union of Chambers of Turkish Engineers and Architects, Istanbul Branch of Chamber of Civil Engineers, Istanbul.
XTRACT-V.3.0.5, Cross-Sectional X Structural Analysis of Components, Imbsen & Associates Inc., California.